5

Equisalience Analysis: A New Window Into the Functional Architecture of Human Cognition

Charles E. Wright, Charles Chubb, Alissa Winkler, and Hal S. Stern

Different dimensions of visual sensitivity play different roles in visual processing. We see this neurophysiologically in the specialization of brain regions for various sorts of visual information. For example, as discussed in this chapter, the magnocellular layers of the lateral geniculate nucleus (LGN) convey information about achromatic luminance variations of low spatial and high temporal frequency, whereas the parvocellular layers carry information about both chromatic and achromatic variations of high spatial and low temporal frequency (Livingstone & Hubel, 1987, 1988). Psychophysics also reveals that different sorts of visual information play different roles in visual processing. Consider that acuity for luminance modulations is much higher than acuity for either (a) equiluminant, chromatic modulations (e.g., Mullen, 1985) or (b) modulations of texture contrast (Sutter, Sperling, & Chubb, 1995). Apparently, variations in light intensity (compared with variations in color or in texture contrast) have special status in conveying information about fine detail in the visual scene. By contrast, Chaparro, Stromeyer, Huang, Kronauer, and Eskew (1993) investigated detection of briefly flashed, small (between 5′ and 15′ of arc) foveally presented spots; spots could differ from the background either in color (either redder or greener than the yellow background) or in luminance (either brighter or darker than the background). Over the range of spot sizes and durations tested, participants were generally more sensitive to chromatic than to luminance differences, leading Chaparro et al. to claim in their title that "Colour is what the eye sees best" (p. 348). They also concluded, based on differences in temporal and spatial summation, that different signal processing streams are used to produce the luminance and chromatic judgments.

These considerations suggest that to understand human visual processing, we need to understand what sorts of visual information (which dimensions of

DOI: 10.1037/14135-006
Human Information Processing: Vision, Memory, and Attention, C. Chubb, B. A. Dosher, Z.-L. Lu, and R. M. Shiffrin (Editors)

visual sensitivity) are used for what computational purposes. The main goal of this chapter is to introduce equisalience analysis (EA), a psychophysical method to address this question, likely to find applications in diverse areas of human perception and cognition. To motivate and explain the approach, we have chosen an example that has generated substantial recent interest: characterizing the differences in visual what-and-where processing.

The idea that visual processing splits into anatomically and functionally distinct dorsal and ventral streams originates with Ungerleider and Mishkin (1982), who called them the *where* and *what* streams because they thought the function of the dorsal stream was to localize things in space whereas that of the ventral stream was to identify things. They also pointed out that these streams receive their primary input from different subcortical pathways. Although both streams receive input from the magnocellular layers of the LGN, the ventral stream alone also receives input from the parvocellular layers.

These two subcortical streams carry different sorts of information (Livingstone & Hubel, 1988). Neurons in the parvocellular layers tend to be color-selective and sluggish with small receptive fields. By contrast, magnocellular neurons tend to be insensitive to color and fast (sensitive to rapid transients) with large receptive fields. These observations suggest that dorsally mediated functions might be less sensitive to color variations than ventral functions.

Since Ungerleider and Mishkin's (1982) original what-and-where theory, alternative theories of ventral–dorsal visual processing have been proposed. The most influential of these is the *what-and-how* theory of Milner and Goodale (1995), who argued that the ventral stream is specialized "to permit the formation of perceptual and cognitive representations that embody the enduring characteristics of objects and their significance," whereas the dorsal stream "mediate(s) the control of goal-directed movements" using primarily "instantaneous and egocentric features of objects" (p. 66). Others (e.g., Creem & Proffitt, 2001) have argued for a hybrid *what–where–how* theory that locates the *where* system in the inferior parietal lobule and the *how* system in the superior parietal lobule.

Many studies have attempted to demonstrate a functional difference in the processing of visual information by tasks thought to be primarily "dorsal" versus "ventral." One approach has been to look for evidence of visual "illusions" in ventrally mediated judgment tasks and the relative absence of such illusions in dorsally mediated pointing or grasping tasks (e.g., Aglioti, Goodale, & DeSouza, 1995; Brown, Moore, & Rosenbaum, 2002; Haffenden & Goodale, 1998, 2000; Haffenden, Schiff, & Goodale, 2001). However, as witnessed by the debate over this issue (Franz, 2001; Franz, Buelthoff, & Fahle, 2003; Franz, Fahle, Buelthoff, & Gegenfurtner, 2001; Franz, Gegenfurtner, Buelthoff, & Fahle, 2000; Smeets & Brenner, 2006), these studies have failed to provide comparisons that compellingly demonstrate a functional difference. In a recent review of this and other related lines of evidence, Cardoso-Leite and Gorea (2010) suggested that this distinction may be impossible to "test" definitively because of "pervasive methodological problems relating precisely to the empirical (im)possibility of 'strictly matching' perceptual and motor tasks" (p. 133). An important part of this problem is that the tasks being compared have different dependent measures. Even using tasks with dependent variables that have the same units (e.g., the latency

of a judgment and the duration of a movement, both measured in milliseconds) does not solve the underlying "apples and oranges" problem.

We propose EA as a way to overcome these inherent problems in comparing the relative sensitivity of two or more tasks to visual stimulation. We present EA first conceptually and then with a set of illustrative, but real, data.

Equisalience Analysis

To appreciate the issues involved in comparing data across tasks, consider a thought experiment modeled after one of the experiments that we have actually run. (We present some actual, illustrative data later.) This thought experiment includes two blocked tasks: a speeded identification task and a masked location task. (Under the what-and-where theory, one might expect the identification and location tasks to selectively engage the ventral and dorsal streams, respectively.) The stimuli for both tasks are identical: an isosceles triangle pointing in one of four directions—up, down, right, or left—presented at one of four locations. In the masked location task, the stimulus is masked after a brief display, and the participant presses one of four keys to indicate the location of the triangle. In the speeded identification task, the stimulus remains visible, and the participant presses one of four keys as quickly as possible to indicate which way the triangle is pointing.

In each task, the target can be defined in either of two ways: It can be gray and brighter than the background, or it can be green and equiluminant to the background. In either case, the target also varies from trial to trial in intensity—that is, in luminance for gray targets or in saturation for green targets. In the masked location task, the dependent variable is proportion of correct responses; in the speeded identification task, it is response time.

Under the what-and-where theory, one might expect the identification task to draw mainly on ventral and the location task on dorsal processes. If so, then one might expect the two tasks to have roughly equal sensitivity to luminance variations (both streams get magnocellular input); however, because only the ventral stream gets parvocellular input, one might expect the identification task to be more sensitive to equiluminant green variations than the location task.[1] This leads the what-and-where theorist to predict that these two tasks differ in their relative sensitivity to luminance versus green saturation. The choice of two tasks with very different dependent variables will help to illustrate the strengths of the EA method.

For any given task, T, the gray-to-green equisalience function f_T maps any gray-intensity x onto the green-intensity $y = f_T(x)$ that yields the same level of performance as x. This concept is illustrated for the masked location task, Task 1 on left side of Figure 5.1. The two curves show hypothetical psychometric functions

[1]It should be noted that the equiluminant green stimuli are expected to activate both the parvocellular and koniocellular channels of the LGN. Koniocellular neurons seem to be sensitive primarily to S-cone activations (see Hendry & Reid, 2000, for a review). At the risk of oversimplifying the discussion, we ignore possible complications resulting from the koniocellular channel.

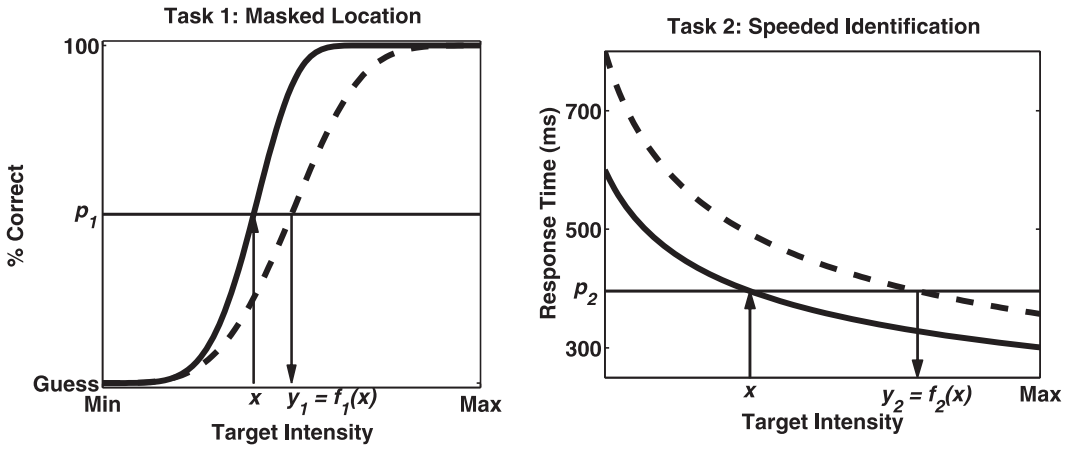

Figure 5.1. Hypothetical data from two tasks. In both panels, task performance is related to target intensity. For Task 1, in the left panel, performance is measured by percent correct; for Task 2, in the right panel, performance is measured by reaction time. In both panels, the solid curve gives performance as a function of target luminance, and the dashed curve gives performance as a function of equiluminant green target saturation. In Task 1, the green saturation value y_1 yields the same level of performance, p_1, in the masked location task as does luminance x. This means $y_1 = f_1(x)$, where f_1 is the gray-to-green equisalience function for the masked location task; that is, x and y_1 are equisalient for this task. In Task 2, the green saturation value y_2 yields the same level of performance, p_2, in the masked location task as does luminance x; that is, x and y_2 are equisalient for this Task 2.

from this task, one for gray intensities (solid line) and one for green (dashed line). The horizontal line indicates the performance level p_1 yielded by gray-intensity x. This line intersects the green psychometric function at point $y_1 = f_1(x)$, for f_1, the gray-to-green equisalience function for the masked location task.

Analogous, hypothetical, speeded identification task data are shown for Task 2 on the right side of Figure 5.1. Notice that the dependent measure is different from that of Task 1; nonetheless, we can define the gray-to-green equisalience function f_2 just as we defined f_1. That is, gray-intensity x maps to a performance level p_2, which maps to the corresponding green-intensity $y_2 = f_2(x)$.

Figure 5.2 makes it clear that the location and identification tasks differ. Here the circle and square mark the equisalient points in a coordinate system with gray intensity on the horizontal and green on the vertical axis: the circle marks the equisalient point from Task 1 (x, y_1), the location task, and the square marks the equisalient point from Task 2 (x, y_2), the identification task. In this hypothetical example, levels of gray and green intensity that yield identical location task performance (x and y_1) yield different identification-task performance: A higher green intensity (y_2) is required to produce the same identification-task performance as x. This difference, which we call a *task-related contrast in sensitivity,* is important because we might suppose that, if two tasks with the same information requirements are informed by the same data stream, then any manipulation of the input that influences the quality of the data available in that stream should analogously influence performance in both tasks, in

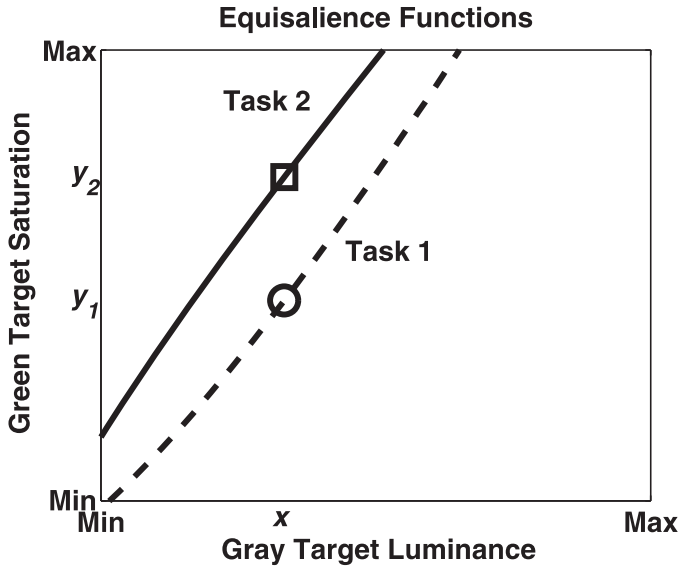

Figure 5.2. Hypothetical equisalient points and functions of luminance and saturation for two tasks. The two points, marked by a circle and a square, are equisalience points. Each indicates the level of green target saturation (y_1 for Task 1, the masked location identification task, and y_2 for Task 2, the speeded shape identification task) that produces the same level of performance as a gray target luminance level, x. The two curves are equisalience functions that generalize the relationship indicated by the equisalience points across the range of gray target luminance levels. The dashed line is for Task 1. The solid line is for Task 2.

which case we would have observed the same equisalient point for both tasks. Figure 5.2 contradicts this expectation for manipulations of gray and green across the location and identification tasks, suggesting either that they have different information requirements or that they do not reside in the same data stream.

EA is an elaboration of the procedure just described for comparing equisalient points. A minimal application of EA involves two dimensions of stimulus intensity, X and Y (e.g., luminance and green saturation), and two tasks, $Task_1$ and $Task_2$ (e.g., the speeded identification and masked location tasks). The first step is to collect data using various levels of each of X and Y in each of tasks $Task_1$ and $Task_2$. We then use standard models to fit the X-data in $Task_1$, the Y-data in $Task_1$, the X-data in $Task_2$ and the Y-data in $Task_2$, in each case deriving a parametric function relating stimulus intensity to performance. In the foregoing example, data would be collected to fit the four functions shown in Figure 5.1. Then for each of $k = 1$ and 2, we use the parameters from the fits of X-data and Y-data in $Task_k$ to derive the $Task_k$, X-to-Y equisalience function f_k. To reiterate, for any X-intensity x, $f_k(x)$ gives the Y-intensity that yields the same level of performance as x in $Task_k$. The two lines in Figure 5.2 are the equisalience functions for the masked location and speeded identification tasks, the psychophysical functions of which are shown in Figure 5.1. Importantly, the X-to-Y equisalience function for a task does not depend on the measure of performance used in the task.

As shown in Figure 5.2, visual comparison of the equisalience functions strengthens the impression that variations of X = gray and Y = green intensities influence performance differently in the two tasks. However, for EA to be a useful tool, it is important that we go beyond visual impressions and provide a statistical test of the null hypothesis that the X-to-Y equisalience functions of the two tasks are equal. Here, if one makes standard assumptions about the relation of stimulus intensity to performance, the equisalience functions for both forced-choice and speeded tasks turn out to be power functions. That is, for either sort of task, the X-to-Y equisalience function takes the form $f(x) = \gamma x^{\phi}$, where the parameters γ and ϕ can be computed from the parameters used to fit the X- and Y-data from that task. This result enables a straightforward likelihood-ratio test of the null hypothesis that the X-to-Y equisalience functions of the two tasks are identical, that is, they have the same values of γ and ϕ.

To summarize, EA is a new method for testing whether cognitive processes have similar access to or make equivalent use of different sorts of sensory information. This method requires (a) two (or more) to-be-compared tasks,[2] in each of which performance depends on the sensory strength of the stimulus information; (b) two (or more) sensory stimulus dimensions; and (c) an invertible function relating intensity to performance for each task, such that the resulting equisalience function can be parameterized with the same function, here a power function. EA does not replace psychometric functions as an important way to understand performance with different tasks and stimulus dimensions. What the method provides is a systematic way to compare the relative sensitivity of different tasks to different dimensions of stimulus intensity.

Equisalience Functions Versus Equisalience Points

A reasonable question at this point is whether it is necessary to develop full equisalience functions to make these comparisons. After all, in our development of equisalience functions, we alluded to drawing the inferences of interest simply by comparing equisalience points. As described later, we have found the concept of equisalience functions has helped to clarify this issue.

An approach based on the analysis of equisalient points seems particularly plausible as an extension of a technique often used to compare psychophysical data across conditions. A nice example of this technique is a paper by Pestilli and Carrasco (2005) that looked at the effect of valid, neutral, and invalid cues (which we can think of as three different tasks) on the discrimination of the orientation of Gabor patches at two eccentricities. To make these comparisons, they used a staircase procedure to estimate the stimulus contrast needed to achieve 82% correct responses (so contrast at Eccentricity 1 plays the role of x, and contrast at Eccentricity 2 plays the role of y). If the valid-cue task is Task 1 and the invalid-cue task is Task 2, then this procedure yields equisalient pairs (x_1, y_1) for Task 1 and (x_2, y_2) for Task 2. The panels of Figure 5.3 illustrate pairs

[2]For convenience and brevity, we have chosen always to describe these comparisons as being between "tasks." However, there is nothing in the logic of EA that prohibits it from being used to compare salience across what might be considered "conditions" within a single task.

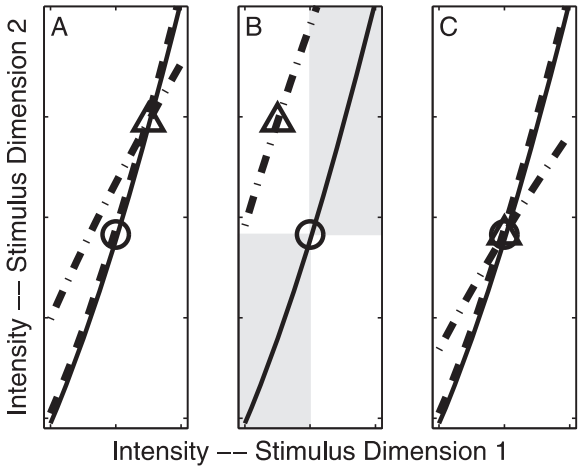

Figure 5.3. Three possible outcomes for an experiment with only one equisalient point for each task.

of equisalient points from three possible outcomes from such an experiment and several equisalience functions consistent with each outcome. The horizontal and vertical axes in Figure 5.3 represent stimulus intensity on each of two stimulus dimensions. The circle, in each panel, indicates the equisalient point for Task 1, that is, the pair of intensities that produced criterion performance in this task. The triangle indicates the equisalient point for Task 2.

Panel A of Figure 5.3 illustrates a plausible outcome in which the equisalient points differ, on both stimulus dimensions. The solid line is an equisalience function (one of many) consistent with the equisalient point for Task 1. The two broken lines are both consistent with the equisalient point for Task 2. The figure makes the ambiguity in this outcome obvious: These two equisalient points can arise either when there truly is a task-related contrast in sensitivity or when there is not such a difference. In the first case, the equisalience function for Task 2 might be the broken line with the dot-dash pattern. If there is no difference, the equisalience function for Task 2 must be the dashed line that is collinear with the solid line that is the equisalience function for Task 1.

One clear difference between the outcome illustrated in Panel A of Figure 5.3 and that of Figure 5.2 is that the procedure for generating the equisalient points in Figure 5.2 included steps designed to ensure that the same stimulus intensity level was used to generate the data on one of the stimulus dimensions (the one represented by the horizontal axis in Figure 5.2) for both tasks. As a result, both equisalient points were constrained to fall on a single vertical line. Perhaps this constraint is necessary to produce results that can be interpreted without ambiguity.

Panel B of Figure 5.3 shows that it is possible, however, to obtain equisalient points that can be interpreted unambiguously with a less restrictive constraint. In Panel B, the equisalient points again differ. However, because equisalience functions are power functions and must be monotonically increasing, there is no equisalience function that can pass through both of these two equisalient points, and thus there is no ambiguity: They must reflect a task-related contrast

in sensitivity. We can reach this same conclusion (up to the limits of statistical reliability) if the equisalient point for Task 2 lies anywhere in the unshaded region of Panel B. This shows that a single pair of equisalient points can suffice to demonstrate the existence of a task-related contrast.

By contrast, however, Panel C of Figure 5.3 makes it clear that a single pair of equisalient points can never refute the existence of a task-related contrast. In this case, the equisalient points for the two tasks lie on top of one another. This is the case when the criterion performance level is produced by the same pair of stimulus intensities in Task 1 and Task 2. In the discussion of Figure 5.2, we implied that this outcome was consistent with the absence of a task-related contrast. However, as the three equisalience functions in Panel C make clear, this result is ambiguous: If the solid line is the equisalience function for Task 1, the equisalience function for Task 2 can be either collinear (the dashed line) or not (the broken line with the dot-dash pattern). Resolution of this ambiguity requires data defining at least two separated equisalient points for each task. Although it might be marginally more efficient to limit one's data to just that necessary to satisfy this requirement, in fact, the data required to fit both full psychometric functions for each task, and thus to determine the equisalience functions, is not that much more extensive than the data required to precisely estimate two equisalient points for each task.

Treatment of Actual Data

Tasks and Stimuli

To illustrate the application of EA, this section briefly describes an actual experiment that builds on the thought experiment described in the previous section. In this experiment, data from three tasks using the same stimuli, and six levels each of gray luminance and green saturation were collected for each of eight trained participants over five daily, 1-hour sessions (following 4 days of practice). The stimulus on each trial was one of four isosceles triangles (Figure 5.4b shows an upward gray version) displayed at one of four parafoveal locations about a fixation mark (Figure 5.4a).

In the speeded location task, participants pressed one of four keys as quickly as possible to indicate target location (Figure 5.4b); the stimulus stayed on until the response. The masked location task was similar except that the screen was masked 116 ms after stimulus onset, and participants guessed target location without worrying about speed. In the speeded identification task, participants pressed a key (Figure 5.4c) to indicate which way the target triangle was pointing; there was no mask. For both speeded tasks, errors were excluded from the analysis.

The target on a given trial differed from the gray background (CIE coordinates $Y = 23.4$ cd/m^2, $x = .293$, $y = .303$) in either luminance or color. Based on results during the practice days, six levels of gray target luminance ($24.3 \leq x \leq 25.4$) and equiluminant green target variation ($.328 \leq y \leq .371$) were chosen for each participant to yield performance ranging from 30% to 95% correct in the masked location task. It should be noted that although the primary variation in the green target is in its saturation, it also varies in hue.

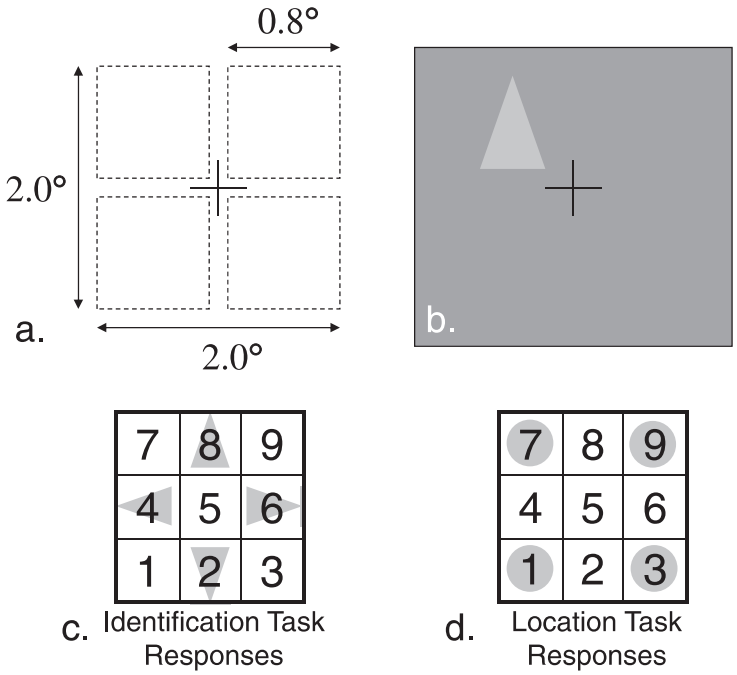

Figure 5.4. Stimuli and response layouts used in the experiment. Part a shows the dimensions of the array containing four possible stimulus locations. Part b shows possible stimulus, illustrating a single level of location, shape, luminance, for a gray target (not shown saturation of green targets). Part c shows how stimulus shape was mapped to response keys in the identification task. Part d shows how stimulus location was mapped to the response keys in the location task.

Rationale

The what-and-where theory predicts that the two location tasks should rely on dorsal mechanisms, whereas under the what-and-how theory, the judgments required in the location tasks are of allocentric position and thus should be ventrally mediated, although perhaps localized in the inferior parietal lobule. Under both theories, speeded identification should be ventrally mediated. Thus, the what-and-how theory predicts that the gray-to-green equisalience functions of all three tasks will be the same; however, the what-and-where theory predicts that the gray-to-green equisalience function for the identification task will differ from those of the two location tasks. In any case, if (as seems likely) the masked and speeded location tasks are mediated by one mechanism, then their gray-to-green equisalience functions should be the same.

Results

Figure 5.5 shows, for one participant, three equisalience functions with the fitted data, one for each of the tasks. For any level p of performance in a given task, T, there exists a unique luminance $x(p)$ and saturation $y(p) = f_T(x(p))$, that yield performance p. Each of the three equisalience functions in Figure 5.5

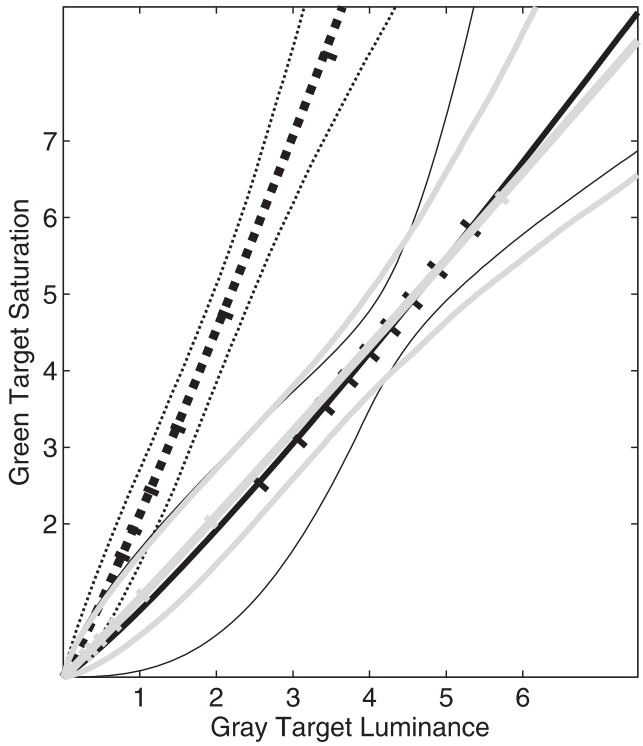

Figure 5.5. Equisalience functions of green saturation versus luminance for three tasks from one participant. The dotted black line is the equisalience function for the speeded, shape identification task. The solid black line is the equisalience function for the speeded location task. The solid gray line is the equisalience function for the masked location task. The tick marks along the gray line (masked location task) mark nine equisalience points that range from a proportion correct of 0.325, at the lower to 0.925, on the upper right, in steps of 0.075. The tick marks along the solid black (speeded shape) and dotted black (speeded location) lines mark six equisalience points that range from a reaction time of 1000 ms, on the lower left, to 500 ms, on the upper right, in 100 ms increments.

plots the locus of points $(x(p), y(p))$ for a task. Notice that the dependent measure, p, has no explicit representation in Figure 5.5, although we could label every point on any equisalience function with the corresponding value of p. As indicated in the figure caption, tick marks on each equisalience function locate specific, arbitrary performance levels.

The implicit representation of p creates a problem; it makes it difficult to indicate the dispersion of the actual data around the model predictions. This problem is solved in Figure 5.5 by contour lines surrounding each equisalience function marking 95% credible intervals obtained using a Bayesian procedure.

Note that for this participant (a) the equisalience functions for the speeded location (solid black line) and masked location (solid gray line) tasks are nearly identical, whereas (b) the equisalience function for the identification task (dotted black line) differs strongly from those for the two location tasks. As shown in Table 5.1, this pattern reflects a general tendency observed across our participants. Specifically, for six of our eight observers, a likelihood ratio

Table 5.1. Summaries of Two Paired-Task Comparisons

	Speeded location vs. masked location			Speeded identification vs. masked location		
	Likelihood ratio test			Likelihood ratio test		
Subject	χ^2	p	Log_{10} Bayes factor	χ^2	p	Log_{10} Bayes factor
1	1.38	.502	1.544	52.86	.000	–4.014
2	0.18	.938	1.908	90.94	.000	–10
3	9.34	.009	–0.911	64.11	.000	–4.706
4	2.34	.309	1.465	62.54	.000	–3.954
5	8.43	.014	–0.003	27.74	.000	–2.038
6	2.66	.265	1.978	122.37	.000	–10
7	4.35	.113	1.819	72.86	.000	–3.233
8	0.43	.808	2.034	104.86	.000	–10

test (method described later) fails to reject the null hypothesis that the equisalience functions for the masked and speeded versions of the location task are different. (Consonant with this result, Bayes factors strongly favor equality of the equisalience functions for the two location tasks.) By contrast, for all eight observers, likelihood ratio tests decisively reject the null hypothesis that the equisalience functions for the identification task and masked location task are equal ($p < .0001$ in all cases, and all of the log-Bayes factors are less than –2).

Discussion

The finding that the equisalience functions are similar for the masked and speeded location tasks confirms our expectation that, despite the change in dependent variable associated with the change from a speeded- to an accuracy-based procedure, these two tasks are mediated by the same processes. The result that equisalience functions are different for the masked location versus the identification task might be taken to confirm the what-and-where theory in favor of the what-and-how theory of ventral–dorsal processing. However, as Cardoso-Leite and Gorea (2010) so persuasively argued, the results from any single EA experiment are unlikely to support conclusions as strong as this. An alternative account of the current results, for example, proposes that the identification task makes use of higher spatial frequency information than do the location tasks (because high spatial frequencies are required to discriminate the tip of the isosceles triangle from the other vertices). Therefore, because high spatial frequency information is carried more efficiently by luminance than by equiluminant chromatic variations, the identification task is relatively less sensitive to saturation versus luminance than the location tasks. Additional EA experiments are needed to determine exactly why the equisalience functions for the identification and location tasks differ, but this is an ambiguity inherent in understanding a complex system, not a problem of the method.

Testing the Hypothesis that Two Tasks Share the Same Equisalience Function

In the previous section, we reported *p* values for two tests of the null hypothesis that two equisalience functions are identical. This section explains how the equisalience functions and these *p* values were obtained.

The Models for the Forced-Choice and Response-Time Tasks

We first derive the equisalience functions for the two psychometric models used to address performance in the tasks of interest: the model for a four-alternative forced-choice (4-AFC) task (e.g., the masked location task) and the model for a response-time task (e.g., the speeded location or the speeded identification task). For concreteness, we continue to use x for target luminance and y for equiluminant green target saturation; however, x and y could be variable intensities of any sensory properties.

We model 4-AFC task performance using Weibull functions (Mortensen, 2002; Quick, 1974):

$$\Psi(u|\alpha,\beta) = .25 + .75\left(1 - e^{-\left(\frac{u}{\alpha}\right)^{\beta}}\right). \qquad (5.1)$$

For some α_L, β_L, α_S, and β_S, probability correct is assumed to be $\Psi(x \mid \alpha_L, \beta_L)$ for a gray target of luminance x and $\Psi(y \mid \alpha_S, \beta_S)$ for a green target of saturation y. Under these assumptions, the equisalience function for the 4-AFC task is

$$f_1(x) = \Psi_S^{-1}(\Psi_L(x)) = \gamma_1 x^{\phi_1}, \qquad (5.2)$$

where

$$\gamma_1 = \frac{\alpha_S}{\alpha_L^{\left(\frac{\beta_L}{\beta_S}\right)}} \text{ and } \phi_1 = \frac{\beta_L}{\beta_S}. \qquad (5.3)$$

When viewed in the form of Equation 5.2, the equisalience function approach can be seen to be related to the quantile-comparison function used to compare two probability distributions (Lehmann, 1974).

To fit the data from a response-time task, we assume that, for a given target luminance (or equiluminant green saturation) u, response times w conform to a delay-shifted Wald density:

$$g(w|u,\kappa,\eta,\rho,\delta) = \frac{\rho}{\sqrt{2\pi(w-\delta)^3}} \exp\left[-\left(\frac{(\rho - \kappa u^{\eta}(w-\delta))^2}{2(w-\delta)}\right)\right]. \qquad (5.4)$$

Variants of the Wald distribution are commonly used to model response times (Heathcote, 2004; Luce, 1986). With $\delta = 0$, the Wald distribution reflects the distribution of first-passage times through level ρ of a homogeneous Wiener diffusion process with initial value 0, drift κu^{η}, and variance 1. The idea is

that response time depends on a process of information-accrual that can be mimicked by such a diffusion process. Setting $\delta > 0$ introduces a fixed delay reflecting factors such as sensory transduction and response production. We assume that for a gray target with luminance x, response times have density $g(w|x, \kappa_L, \eta_L, \rho, \delta)$, whereas for a green target with saturation y, response times have density $g(w|y, \kappa_S, \eta_S, \rho, \delta)$. The boundary ρ and delay δ are assumed to be the same for green and gray targets.

Note that $g(w|y, \kappa_S, \eta_S, \rho, \delta) = g(w|x, \kappa_L, \eta_L, \rho, \delta)$ if and only if $\kappa_S y^{\eta_S} = \kappa_L x^{\eta_L}$, implying that

$$f_2(x) = \gamma_2 x^{\phi_2}, \qquad (5.5)$$

where

$$\gamma_2 = \left(\frac{\kappa_L}{\kappa_S}\right)^{\frac{1}{\eta_S}} \text{ and } \phi_2 = \frac{\eta_L}{\eta_S}. \qquad (5.6)$$

Modeling the Equality of Two Equisalience Functions

Equations 5.2 and 5.5 show that for both the forced-choice and response-time models the equisalience functions are power functions. Our unconstrained model allows all parameters from both tasks to vary freely. However, our constrained model requires that $f_1 = f_2$, implying that

$$\gamma_1 = \gamma_2 = \gamma \text{ and } \phi_1 = \phi_2 = \phi, \qquad (5.7)$$

yielding a new parameterization that replaces η_S, β_S, κ_S, and α_S with γ and ϕ by setting

$$\eta_S = \frac{\eta_L}{\phi}, \beta_S = \frac{\beta_L}{\phi}, \kappa_S = \frac{\kappa_L}{\gamma^{\eta_S}} = \frac{\kappa_L}{\gamma^{\left(\frac{\eta_L}{\phi}\right)}}, \text{ and } \alpha_S = \gamma \alpha_L^{\phi}. \qquad (5.8)$$

Thus, the unconstrained model has separate α, β, η, κ parameters for the two tasks, whereas in the constrained model the α, β, η, κ parameters for saturation are derived from ϕ, γ and the parameters for luminance using Equation 5.8.

The 4-AFC Task Likelihood Functions

For any luminance x, let N_x be the number of trials in which the target had luminance x, and let k_x be the number of those N_x trials in which the observer responded correctly. Define N_y and k_y analogously for any green saturation y. Then the 4-AFC task, gray-target-trial, likelihood function is

$$\Lambda_1^L(\alpha_L, \beta_L) = \prod_x \Psi(x|\alpha_L, \beta_L)^{k_x} (1 - \Psi(x|\alpha_L, \beta_L))^{N_x - k_x}, \qquad (5.9)$$

where the product in Equation 5.9 is over all luminances x used to define targets in the task. Similarly, the green-target-trial likelihood function is

$$\Lambda_1^S(\alpha_S,\beta_S)=\prod_y \Psi(y|\alpha_S,\beta_S)^{k_y}(1-\Psi(y|\alpha_S,\beta_S))^{N_y-k_y}, \qquad (5.10)$$

where the product in Equation 5.10 is over all saturations y used to define green targets in the task.

The Response-Time Task Likelihood Functions

Let w_t be the response time on trial t in the response-time task; if the target on trial t was gray, let x_t be its luminance; if green, let y_t be its saturation. Then the gray- and green-target-trial likelihood functions are

$$\Lambda_2^L(\kappa_L,\eta_L,\rho,\delta)=\prod_{\text{gray-target trials } t} g(w_t|x_t,\kappa_L,\eta_L,\rho,\delta), \qquad (5.11)$$

and

$$\Lambda_2^S(\kappa_S,\eta_S,\rho,\delta)=\prod_{\text{green-target trials } t} g(w_t|y_t,\kappa_S,\eta_S,\rho,\delta). \qquad (5.12)$$

The Likelihood Functions for Both Tasks

For any α_L, β_L, α_S, β_S, κ_L, η_L, κ_S, η_S, ρ, and δ, the likelihood function for the results of both tasks is

$$\Lambda_{Unconstrained}(\alpha_L,\beta_L,\alpha_S,\beta_S,\kappa_L,\eta_L,\kappa_S,\eta_S,\rho,\delta)=$$
$$\Lambda_1^L(\alpha_L,\beta_L)\Lambda_1^S(\alpha_S,\beta_S)\Lambda_2^L(\kappa_L,\eta_L,\rho,\delta)\Lambda_2^S(\kappa_S,\eta_S,\rho,\delta). \qquad (5.13)$$

In the constrained model,

$$\Lambda_{Constrained}(\phi,\gamma,\alpha_L,\beta_L,\kappa_L,\eta_L,\rho,\delta)=$$
$$\Lambda_{Unconstrained}(\alpha_L,\beta_L,\alpha_S,\beta_S,\kappa_L,\eta_L,\kappa_S,\eta_S,\rho,\delta), \qquad (5.14)$$

where the values of η_S, β_S, κ_S and α_S appearing on the right are given by Equation 5.8.

As is well known (e.g., Hoel, Port, & Stone, 1971), if the null hypothesis that $f_1 = f_2$ is true, then the statistic

$$X=-2\ln\left(\frac{\max(\Lambda_{Constrained})}{\max(\Lambda_{Unconstrained})}\right) \qquad (5.15)$$

is asymptotically distributed as chi-square with two degrees of freedom (for the two additional parameters used in the unconstrained model).

Bayesian Elaborations of Equisalience Analysis

We have described traditional likelihood-based inference for equisalience functions; however, a Bayesian approach offers important benefits. First, one can incorporate previous information about the parameters used for the tasks and properties being compared. Although investigators are unlikely to impose strong prior constraints, they may wish to provide upper or lower bounds (or both) on model parameters based on results in the literature. Second, the Bayesian approach frees us from large sample inference. Modern, simulation-based (Markov chain Monte Carlo) methods enable accurate posterior inferences for any sample size, providing posterior intervals for individual psychophysical model parameters. Also, because the equisalience function parameters are functions of the psychophysical model parameters, posterior inference is available for the equisalience functions as well. Finally, the Bayesian approach facilitates hierarchical modeling to accommodate multiple subjects in a single analysis.

In the current study, we used Bayesian parameter estimation (Markov chain Monte Carlo simulation) to generate credible intervals around equisalience function plots in Figure 5.5. This provides a convenient (if indirect) way of indicating the dispersion of the data around model estimates. In addition, we use the Savage–Dickey (e.g., Verdinelli & Wasserman, 1995) method to derive Bayes factors (Columns 3 and 6 of Table 1) comparing the constrained model requiring equisalience functions to be equal to the unconstrained model. For purposes of comparing these Bayes factors to the results of the likelihood ratio tests, note that any Bayes factor whose log (base 10) is greater than 1.0 (–1.0) is typically taken as strong evidence in favor of the constrained (unconstrained) model. It is easy to see that the Bayesian tests return results that are highly consonant with the likelihood ratio tests.

Summary of Fitting Procedures

In this example, different models are appropriate to summarize the data yielded by response-time and 4-AFC tasks (Wald vs. Weibull distributions). Nonetheless, these two models both yield equisalience functions of the same form (power functions). Consequently, the null hypothesis that two tasks of either type share the same equisalience function nests within the general model in which all parameters vary freely. This enables a comparison of these hypotheses that can be done, as we have spelled out, using likelihood ratio test or a Bayes factor.

We emphasize that EA can be used to compare any two tasks, provided that their equisalience functions are both of the same form. Thus, the method is straightforward if the dependent variables of the two tasks are identical. However, as illustrated here, the method can often be applied to compare tasks with different dependent variables.

Summary

EA is a new method for analyzing the functional architecture of human perception and cognition. EA allows one to compare the relative sensitivity of two or more perceptual–cognitive tasks to two or more dimensions of stimulus intensity.

For a given task T, and two dimensions X and Y of stimulus intensity that can be used to control performance in T (e.g., X might be luminance and Y equiluminant green saturation), the X-to-Y equisalience function f_T maps any intensity x of X onto the intensity $y = f_T(x)$ of Y that yields the same level of performance in task T. Here we have shown how to test statistically whether two tasks (possibly with different dependent variables) share the same X-to-Y equisalience function. This question is of interest because, if two tasks with the same information requirements are found to have different equisalience functions, then the tasks probably reside in different processing streams. There are two primary ways of using EA to make scientific progress. First, by discovering tasks with different equisalience functions, we can begin to analyze cognitive processing into different functional streams. Second, by enlarging families of tasks that all share the same equisalience function, we can delineate the functional boundaries between those streams.

References

Aglioti, S., Goodale, M. A., & DeSouza, J. F. X. (1995). Size-contrast illusions deceive the eye but not the hand. *Current Biology, 5,* 679–685. doi:10.1016/S0960-9822(95)00133-3

Brown, L. E., Moore, C. M., & Rosenbaum, D. A. (2002). Feature-specific perceptual processing dissociates action from recognition. *Journal of Experimental Psychology: Human Perception and Performance, 28,* 1330–1344. doi:10.1037/0096-1523.28.6.1330

Cardoso-Leite, P., & Gorea, A. (2010). On the perceptual/motor dissociation: A review of concepts, theory, experimental paradigms and data interpretations. *Seeing and Perceiving, 23,* 89–151. doi:10.1163/187847510X503588

Chaparro, A., Stromeyer, C. F., III, Huang, E. P., Kronauer, R. E., & Eskew, R. T. (1993). Color is what the eye sees best. *Nature, 361,* 348–350. doi:10.1038/361348a0

Creem, S. H., & Proffitt, D. R. (2001). Defining the cortical visual systems: "What," "where," and "how." *Acta Psychologica, 107,* 43–68. doi:10.1016/S0001-6918(01)00021-X

Franz, V. H. (2001). Action does not resist visual illusions. *Trends in Cognitive Sciences, 5,* 457–459. doi:10.1016/S1364-6613(00)01772-1

Franz, V. H., Buelthoff, H. H., & Fahle, M. (2003). Grasp effects of the Ebbinghaus illusion: Obstacle avoidance is not the explanation. *Experimental Brain Research, 149,* 470–477.

Franz, V. H., Fahle, M., Buelthoff, H. H., & Gegenfurtner, K. R. (2001). Effects of visual illusions on grasping. *Journal of Experimental Psychology: Human Perception and Performance, 27,* 1124–1144. doi:10.1037/0096-1523.27.5.1124

Franz, V. H., Gegenfurtner, K. R., Buelthoff, H. H., & Fahle, M. (2000). Grasping visual illusions: No evidence for a dissociation between perception and action. *Psychological Science, 11,* 20–25. doi:10.1111/1467-9280.00209

Haffenden, A. M., & Goodale, M. A. (1998). The effect of pictorial illusion on prehension and perception. *Journal of Cognitive Neuroscience, 10,* 122–136. doi:10.1162/089892998563824

Haffenden, A. M., & Goodale, M. A. (2000). Independent effects of pictorial displays on perception and action. *Vision Research, 40,* 1597–1607. doi:10.1016/S0042-6989(00)00056-0

Haffenden, A. M., Schiff, K. C., & Goodale, M. A. (2001). The dissociation between perception and action in the Ebbinghaus illusion: Nonillusory effects of pictorial cues on grasp. *Current Biology, 11,* 177–181. doi:10.1016/S0960-9822(01)00023-9

Heathcote, A. (2004). Fitting Wald and ex-Wald distributions to response time data: An example using functions for the S-PLUS package. *Behavior Research Methods, Instruments & Computers, 36,* 678–694. doi:10.3758/BF03206550

Hendry, S. H. C., & Reid, R. C. (2000). The koniocellular pathway in primate vision. *Annual Review of Neuroscience, 23,* 127–153. doi:10.1146/annurev.neuro.23.1.127

Hoel, P. G., Port, S. C., & Stone, C. J. (1971). *Introduction to statistical theory.* Boston, MA: Houghton-Mifflin.

Lehmann, E. L. (1974). *Statistical methods based on ranks.* San Francisco, CA: Holden-Day.
Livingstone, M., & Hubel, D. (1988, May 6). Segregation of form, color, movement, and depth: Anatomy, physiology, and perception. *Science, 240,* 740–749. doi:10.1126/science.3283936
Livingstone, M. S., & Hubel, D. H. (1987). Psychophysical evidence for separate channels for the perception of form, color, movement and depth. *The Journal of Neuroscience, 7,* 3416–3468.
Luce, R. D. (1986). *Response times.* New York, NY: Oxford University Press.
Milner, A. D., & Goodale, M. A. (1995). *The visual brain in action.* Oxford, England: Oxford University Press.
Mortensen, U. (2002). Additive noise, Weibull functions and the approximation of psychometric functions. *Vision Research, 42,* 2371–2393. doi:10.1016/S0042-6989(02)00195-5
Mullen, K. T. (1985). The contrast sensitivity of human colour vision to red-green and blue-yellow chromatic gratings. *The Journal of Physiology, 359,* 381–400.
Pestilli, F., & Carrasco, M. (2005). Attention enhances contrast sensitivity at cued and impairs it at uncued locations. *Vision Research, 45,* 1867–1875. doi:10.1016/j.visres.2005.01.019
Quick, R. F. (1974). A vector-magnitude model of contrast detection. *Kybernetik, 16,* 65–67. doi:10.1007/BF00271628
Smeets, J. B. J., & Brenner, E. (2006). 10 years of illusions. *Journal of Experimental Psychology: Human Perception and Performance, 32,* 1501–1504. doi:10.1037/0096-1523.32.6.1501
Sutter, A., Sperling, G., & Chubb, C. (1995). Measuring the spatial frequency selectivity of second order texture mechanisms. *Vision Research, 35,* 915–924. doi:10.1016/0042-6989(94)00196-S
Ungerleider, L. G., & Mishkin, M. (1982). Two cortical visual systems. In D. J. Ingle, M. A. Goodale, & R. J. Mansfield (Eds.), *Analysis of visual behavior* (pp. 549–586). Cambridge, MA: MIT Press.
Verdinelli, I., & Wasserman, L. (1995). Computing Bayes factors using a generalization of the Savage-Dickey density ratio. *Journal of the American Statistical Association, 90,* 614–618. doi:10.1080/01621459.1995.10476554